IOP Publishing Journal of Physics A: Mathematical and Theoretical
J. Phys. A: Math. Theor. **46** (2013) 035501 (17pp) doi:10.1088/1751-8113/46/3/035501

Stochastically driven instability in rotating shear flows

Banibrata Mukhopadhyay[1] **and Amit K Chattopadhyay**[2]

[1] Department of Physics, Indian Institute of Science, Bangalore 560 012, India
[2] Non-linearity and Complexity Research Group, Engineering, and Applied Science, Aston University, Birmingham B4 7ET, UK

E-mail: bm@physics.iisc.ernet.in and a.k.chattopadhyay@aston.ac.uk

Received 30 July 2012, in final form 14 November 2012
Published 21 December 2012
Online at stacks.iop.org/JPhysA/46/035501

Abstract

The origin of hydrodynamic turbulence in rotating shear flows is investigated, with particular emphasis on the flows whose angular velocity decreases but whose specific angular momentum increases with the increasing radial coordinate. Such flows are Rayleigh stable, but must be turbulent in order to explain the observed data. Such a mismatch between the linear theory and the observations/experiments is more severe when any hydromagnetic/magnetohydrodynamic instability and then the corresponding turbulence therein is ruled out. This work explores the effect of stochastic noise on such hydrodynamic flows. We essentially concentrate on a small section of such a flow, which is nothing but a plane shear flow supplemented by the Coriolis effect. This also mimics a small section of an astrophysical accretion disc. It is found that such stochastically driven flows exhibit large temporal and spatial correlations of perturbation velocities and hence large energy dissipations of perturbation, which presumably generate the instability. A range of angular velocity (Ω) profiles of the background flow, starting from that of a constant specific angular momentum ($\lambda = \Omega r^2$; r being the radial coordinate) to a constant circular velocity ($v_\phi = \Omega r$), is explored. However, all the background angular velocities exhibit identical growth and roughness exponents of their perturbations, revealing a unique universality class for the stochastically forced hydrodynamics of rotating shear flows. This work, to the best of our knowledge, is the first attempt to understand the origin of instability and turbulence in three-dimensional Rayleigh stable rotating shear flows by introducing additive noise to the underlying linearized governing equations. This has important implications to resolve the turbulence problem in astrophysical hydrodynamic flows such as accretion discs.

PACS numbers: 47.85.Dh, 95.30.Lz, 47.20.Ib, 47.27.Cn, 05.20.Jj, 98.62.Mw

(Some figures may appear in colour only in the online journal)

1. Introduction

There are certain rotating shear flows which are Rayleigh stable but experimental/observational data suggest that they are turbulent. In the absence of magnetic coupling, such flows are stable under linear perturbation. What drives their instability and the resulting turbulence in the absence of linearly unstable modes? In order to understand a plausible route to hydrodynamic turbulence in such flows, a series of papers was published by different independent groups [1–5]. Based on the 'bypass mechanism' [6–8], those papers showed that such flows exhibit large transient energy growth of linear perturbation. It was argued earlier that the large transient energy growth is indeed responsible for the subcritical transition to turbulence in a plane Couette flow and a plane Poiseuille flow, as seen in the laboratory [9]. In such flows the transient growth increases with increasing Reynolds number (R_e). For example, in a plane Couette flow, the maximum transient growth scales as R_e^2; however, the situation changes drastically when rotational effects come into the picture. The Coriolis force is the main culprit behind this change. It was shown earlier [4, 5, 10] that the rate of increase of transient growth in two-dimensional (insignificant vertical scale height) linearized rotating shear flows with Keplerian angular velocity (Ω) profile ($\Omega \sim r^{-3/2}$; r being the radial coordinate of the flow) decreases greatly compared to those in plane Couette flows, when the maximum growth scales as $R_e^{2/3}$. Furthermore, in three dimensions (with finite height), such transient growth in Keplerian flows is insignificant, independent of the viscosity, to generate any instability and turbulence. However, the three-dimensional Keplerian flow is an important natural flow, which exists in several astrophysical contexts. Interestingly, while some authors [11], based on the prototype experiment consisting of the fluid confined between two corotating cylinders, reported Rayleigh stable rotating shear flow, similar to that of a Keplerian disc, laminar, some others [12] found it to be turbulent. However, the results from direct numerical simulations [13] argue that laboratory flows are indeed hydrodynamically unstable and should become turbulent at low Reynolds numbers. The last author [13] and one of the present authors [14] also showed/argued that the experiments are compromised with undesired effects due to the finite length of the cylinders. Note that some (effective) nonlinear theory [15, 16], revealing a large energy growth of the perturbation (even of finite amplitude), argues for plausible routes to turbulence in three dimensions. Hence, the real challenge is to uncover the mystery of the mismatch between the theory and the observation under linear theory, in the absence of a finite amplitude of perturbation.

As has been argued earlier [10], in three dimensions one is required to invoke extra physics, e.g. external or self-generated noise etc, to reveal large energy growth or even instability in the system. It is needless to mention that real flows must be three-dimensional, e.g. an astrophysical accretion disc must have a thickness, however small it may be; hence rotation plays a significant role in determining the dynamics of the flow. The aim of this work is to investigate the amplification of linear perturbations, which may eventually lead to hydrodynamic instability and then plausible turbulence in certain rotating shear flows supplemented by stochastic fluctuations in three dimensions.

There is a long term association of growing unstable modes generated by perturbed flows with statistical physics. The flow fields perturbed either at the boundary or through external forcing have been shown to produce emergent instabilities [17, 18], altering the scaling structure of the systems. It was shown by Forster *et al* [19] that in the long time large distance asymptotic limit, large non-equilibrium fluctuations in unbounded flows decouple to stabilize the flow. The authors also studied the critical dimension beyond which fluctuations become redundant. However, below that dimension, all the Brownian oscillations perturb the flow in the equilibrium limit. In a follow-up work by De Dominicis and Martin [20], a

further generalization of such 'forced Navier–Stokes flows' was provided, incorporating a range of possibilities for perturbing random forces that are correlated with the Kolmogorov spectrum [21, 22] to redefine the scaling laws in the presence of such stochastic components. Later on, the focus was on studying topical variations in the transport properties of fluids under stochastic perturbations [23]. These works were the precursor to the Kardar–Parisi–Zhang (KPZ) model [24], which studied a differential variant of the Burger field to illuminate the fundamental hydrodynamic instabilities related to the intermittency spectrum [25, 26]. The KPZ model also sheds light on varieties of non-equilibrium phenomena, including fluid flows, bacterial growth, paper burning front, etc (see [27]). All such results were later encapsulated in another illustrative work by Medina *et al* [28], where the effects of varying spatio-temporal correlations were studied on the Burger equation (which is a one-dimensional variant of the Navier–Stokes equation). It also showed for the first time that the statistical field theory could be a legitimate consort of fluid mechanics such that local instabilities seen in fluid flows could often be identified as non-trivial infra-red divergences. All the studies, however, were restricted mostly to trivial/periodic and open/absorbing boundary conditions.

Chattopadhyay and Bhattacharjee [29] applied the randomly stirred model of Navier–Stokes flows constrained by the geometry in a flow involving a three-dimensional *bounded* incompressible fluid perturbed by boundary layer shear. In that work, they considered two relatively shearing flat plates with a layer of fluid sandwiched in between. The effect of the constrained flow is implemented through the stochasticity structure function, which ensures that the symmetry is violated through the noise autocorrelation function, in the problem. Note that the geometry could also be changed to rotating co-axial cylinders [30] for externally impressed shearing forces, essentially bearing the same qualitative imprint. This problem, known as boundary layer turbulence, has recently been revisited experimentally in the laboratory, by generating shear in the flow through a raft of blowing air [31]. A numerical simulation governing large eddies also reveals the same experimentally observed non-inertial effects [32]. Note in a related context that astrophysical observed data indeed argue for the signatures of nonlinearity and chaos in rotating shear flows, more precisely accretion flows [33–35], which further support infall of matter towards black holes [36] and neutron stars [37] due to turbulent viscosity.

In this study, we implement the ideas of statistical physics discussed above for rotating shear flows in order to obtain the correlation energy growth of fluctuation/perturbation and the underlying scaling properties. In the next section, we discuss the equations describing stochastically forced perturbed flows, which are to be solved for this paper's purpose. Subsequently, in section 3 we investigate the temporal and spatial correlations of perturbation in detail, in order to understand the plausible instability in the flows. Finally, we summarize the results with conclusions in section 4.

2. Equations describing forced perturbed accretion flow

As our specific interest lies in hydrodynamic instability and turbulence in the presence of stochastic noise, we recall straight away the Orr–Sommerfeld and Squire equations in the presence of the Coriolis force [4, 5, 10], but supplemented by stochastic noise. They are established by eliminating the pressure from the linearized Navier–Stokes equation with background plane shear $(0, -x, 0)$ neglecting magnetic coupling in the presence of the angular velocity $\Omega \sim r^{-q}$ in a small section of the incompressible flow[3]. Hence, the underlying equations are nothing but the linearized set of hydrodynamic equations combined with the

[3] A magnetized version of the set of equations is given in the appendix.

equation of continuity in local Cartesian coordinates (x, y, z) at an arbitrary time t (see, e.g., [4, 10] for a detailed description of the choice of coordinate in a small section) given by

$$\left(\frac{\partial}{\partial t} - x\frac{\partial}{\partial y}\right)\nabla^2 u + \frac{2}{q}\frac{\partial \zeta}{\partial z} = \frac{1}{R_e}\nabla^4 u + \eta_1(x,t), \tag{1}$$

$$\left(\frac{\partial}{\partial t} - x\frac{\partial}{\partial y}\right)\zeta + \frac{\partial u}{\partial z} - \frac{2}{q}\frac{\partial u}{\partial z} = \frac{1}{R_e}\nabla^2 \zeta + \eta_2(x,t), \tag{2}$$

where u, ζ represent respectively the x-components of the velocity and vorticity perturbation, R_e is the Reynolds number, $\eta_{1,2}$ are the components of the noise arising in the linearized system due to stochastic perturbation, such that $\langle \eta_i(\vec{x}, t)\eta_j(\vec{x}', t')\rangle = D_i(\vec{x})\,\delta^3(\vec{x}-\vec{x}')\,\delta(t-t')\,\delta_{ij}$. Note that equations (1) and (2) describe perturbations in a small section of an accretion flow, which could be expressed in local Cartesian coordinates. The long time, large distance behavior of the velocity correlations is encapsulated in $D_i(\vec{x})$, which is a structure pioneered by Forster *et al* [19]. In the Fourier transformed space, the specific structure of the correlation function $D_i(\vec{k})$ depends on the regime under consideration. It can be shown for all (nonlinear) non-inertial flows [19, 29] that $D_i(k) \sim 1/k^d$, where d is the spatial dimension, without a vertex correction and $D_i(k) \sim 1/k^{d-\alpha}$ with $\alpha > 0$, in the presence of a vertex correction. Note, however, that $D_i(\vec{x})$ is constant for white noise.

We now focus on the narrow gap limit, which otherwise leads to an approximation $x \to L$, when L being the (narrow) size of the shearing box in the x-direction. The appropriate choice of a shearing box has already been described by the previous authors; see, e.g., [5, 10], which we do not repeat here. In brief, in a local analysis one considers a small radially confined region of the flow, while the azimuthal confinement is imposed by a periodic boundary condition. This effectively gives rise to a shearing Cartesian box for geometrically thin flows. We further choose a very small L so that we are essentially interested in an orbit. This is in the same spirit as the celebrated work by Balbus and Hawley [38] who initiated the existence of magneto-rotational-instability with axisymmetric perturbation. One of the motivations behind it is as follows. The presence of turbulence in shearing astrophysical accretion discs is mandatory to generate viscosity therein. It is only the viscosity which helps in transporting the energy–momentum from an outer orbit to an inner orbit leading to the inspiral of matter, giving rise to a differential rotating (shearing) structure of accretion discs. As the aim is to address the origin of such viscosity (which cannot be molecular) for rotating shear flows, choosing x to be fixed is justified.

Hence, in the above discussed framework, we can resort to a Fourier series expansion of u, ζ and η_i as

$$\begin{aligned} u(\vec{x}, t) &= \int \tilde{u}_{\vec{k},\omega}\, \mathrm{e}^{\mathrm{i}(\vec{k}.\vec{x}-\omega t)}\mathrm{d}^3k\,\mathrm{d}\omega, \\ \zeta(\vec{x}, t) &= \int \tilde{\zeta}_{\vec{k},\omega}\, \mathrm{e}^{\mathrm{i}(\vec{k}.\vec{x}-\omega t)}\mathrm{d}^3k\,\mathrm{d}\omega, \\ \eta_i(\vec{x}, t) &= \int \tilde{\eta}_{i\vec{k},\omega}\, \mathrm{e}^{\mathrm{i}(\vec{k}.\vec{x}-\omega t)}\mathrm{d}^3k\,\mathrm{d}\omega, \end{aligned} \tag{3}$$

where $\vec{k}$ and ω respectively represent the wave-vector and angular frequency of perturbation. Substituting them into equations (1) and (2) we obtain

$$\begin{pmatrix} \tilde{u}_{\vec{k},\omega} \\ \tilde{\zeta}_{\vec{k},\omega} \end{pmatrix} = \mathcal{M}\begin{pmatrix} \tilde{\eta}_{1\vec{k},\omega} \\ \tilde{\eta}_{2\vec{k},\omega} \end{pmatrix}, \tag{4}$$

where

$$\mathcal{M} = \begin{pmatrix} \mathcal{M}_1 & \mathcal{M}_2 \\ \mathcal{M}_3 & \mathcal{M}_4 \end{pmatrix}, \tag{5}$$

$$\mathcal{M}_1 = \frac{q^2 R_e(k^2 - \mathrm{i}R_e\omega - \mathrm{i}LR_e k_y)}{-k^2q^2(k^2 - \mathrm{i}R_e\omega - \mathrm{i}LR_e k_y)^2 + 2(q-2)R_e^2k_z^2},$$
$$\mathcal{M}_2 = -\frac{2iqR_e^2k_z}{-k^2q^2(k^2 - \mathrm{i}R_e\omega - \mathrm{i}LR_e k_y)^2 + 2(q-2)R_e^2k_z^2},$$
$$\mathcal{M}_3 = -\frac{\mathrm{i}(q-2)qR_e^2k_z}{-k^2q^2(k^2 - \mathrm{i}R_e\omega - \mathrm{i}LR_e k_y)^2 + 2(q-2)R_e^2k_z^2},$$
$$\mathcal{M}_4 = \frac{k^2q^2R_e(k^2 - \mathrm{i}R_e\omega - \mathrm{i}LR_e k_y)}{k^2q^2(k^2 - \mathrm{i}R_e\omega - \mathrm{i}LR_e k_y)^2 - 2(q-2)R_e^2k_z^2}, \tag{6}$$

when $\tilde{\eta}_{i\vec{k},\omega}$; $i = 1, 2$, are the components of noise in $k-\omega$ space, $k = \sqrt{k_x^2 + k_y^2 + k_z^2}$.

3. Two-point correlations of perturbation

We now look at the spatio-temporal autocorrelations of the flow fields u and ζ [27]. For our purpose, the magnitudes and gradients (scalings) of these autocorrelation functions of perturbations would plausibly indicate noise induced instability, which could lead to turbulence in rotating shear flows.

3.1. Temporal correlation

Assuming $\langle\tilde{\eta}_{1\vec{k},\omega}\,\tilde{\eta}_{2\vec{k},\omega}\rangle = 0$, we obtain the temporal correlations of the velocity, vorticity and gradient of the velocity given below as

$$\langle u(\vec{x},t)\,u(\vec{x},t+\tau)\rangle = C_u(\tau) = \int \mathrm{d}^3k\,\mathrm{d}\omega\,\mathrm{e}^{-\mathrm{i}\omega\tau}\langle\tilde{u}_{\vec{k},\omega}\,\tilde{u}_{-\vec{k},-\omega}\rangle,$$
$$\langle\zeta(\vec{x},t)\,\zeta(\vec{x},t+\tau)\rangle = C_\zeta(\tau) = \int \mathrm{d}^3k\,\mathrm{d}\omega\,\mathrm{e}^{-\mathrm{i}\omega\tau}\langle\tilde{\zeta}_{\vec{k},\omega}\,\tilde{\zeta}_{-\vec{k},-\omega}\rangle,$$
$$\left\langle\frac{\partial u(\vec{x},t)}{\partial x}\,\frac{\partial u(\vec{x},t+\tau)}{\partial x}\right\rangle = C_{\mathrm{d}u}(\tau) = \int \mathrm{d}^3k\,\mathrm{d}\omega\,\mathrm{e}^{-\mathrm{i}\omega\tau}k_x^2\langle\tilde{u}_{\vec{k},\omega}\,\tilde{u}_{-\vec{k},-\omega}\rangle, \tag{7}$$

where τ is the time at which the correlations are to be measured. Now using equations (4), (5), (6) and (7)

$$C_u(\tau) = \int \mathrm{d}^3k\,\mathrm{d}\omega\,\mathrm{e}^{-\mathrm{i}\omega\tau}\big[2D_1q^4R_e^2(k^4 + (R_e\omega + LR_ek_y)^2) + 8D_2q^2R_e^4k_z^2\big]\big/\big[-4(-2+q)^2R_e^4k_z^4 + 4R_e^2q^2(-2+q)k^2k_z^2(k^4 - (R_e\omega + LR_ek_y)^2) - k^4q^4(k^4 + (R_e\omega + LR_ek_y)^2)^2\big]. \tag{8}$$

We further consider the projected hyper-surface for which $k_x = k_y = k_z = k/\sqrt{3}$, without much loss of generality for our purpose. As one of our major interests is to determine the scaling laws, this restriction would not matter. However, this is equivalent to a special choice of initial perturbation, which will affect the magnitude of the correlations. We now perform the ω-integration by computing the poles of the kernel given by

$$\omega_1 = \frac{1}{R_e}\left(\sqrt{\frac{2R_e^2(2-q)}{3q^2} - k^4 + \left(\frac{2\sqrt{2}R_e(2-q)}{\sqrt{3}q}\right)k^2} - \frac{LR_ek}{\sqrt{3}}\right),$$
$$\omega_2 = \frac{1}{R_e}\left(\sqrt{\frac{2R_e^2(2-q)}{3q^2} - k^4 - \left(\frac{2\sqrt{2}R_e(2-q)}{\sqrt{3}q}\right)k^2} - \frac{LR_ek}{\sqrt{3}}\right),$$

$$\omega_3 = -\frac{1}{R_e}\left(\sqrt{\frac{2R_e^2(2-q)}{3q^2} - k^4 + \left(\frac{2\sqrt{2}R_e(2-q)}{\sqrt{3}q}\right)k^2} - \frac{LR_e k}{\sqrt{3}}\right),$$

$$\omega_4 = -\frac{1}{R_e}\left(\sqrt{\frac{2R_e^2(2-q)}{3q^2} - k^4 - \left(\frac{2\sqrt{2}R_e(2-q)}{\sqrt{3}q}\right)k^2} - \frac{LR_e k}{\sqrt{3}}\right). \tag{9}$$

By summing the residues at the appropriate poles in the presence of white noise, we evaluate the magnitude of the frequency part of the integration given by

$$\begin{aligned}\mathrm{RES}_{C_u}(q, R_e, \tau) = {} & \frac{2\sqrt{2}\tau}{\sqrt{3(2-q)}}\frac{\pi R_e}{qk^6}\frac{1}{a^2+b^2}[(bm-an)\sin(a)\cosh(b) \\ & +(am+bn)\cos(a)\sinh(b)],\end{aligned} \tag{10}$$

where

$$a = \sqrt{2\tilde{x} + \sqrt{4\tilde{x}^2 + \tilde{y}^2}}, \quad b = \sqrt{\tilde{x} + \sqrt{4\tilde{x}^2 + \tilde{y}^2}},$$
$$\tilde{x} = -\left[\frac{k^4}{R_e^2} + \frac{2}{3}\left(\frac{(2-q)}{q^2}\right)\right]\tau^2, \quad \tilde{y} = \frac{2}{3}\sqrt{6(2-q)}\left(\frac{k^2}{qR_e}\right)\tau^2,$$
$$m = 2k^2(2-q), \quad n = \sqrt{6(2-q)}\left(\frac{qk^2}{R_e}\right).$$

Hence

$$C_u(\tau) = 4\pi\int_{k_0}^{k_m} \mathrm{d}k\, k^2\, \mathrm{RES}_{C_u}(q, R_e, \tau), \qquad \text{with } D_1 = D_2 = 1, \tag{11}$$

where $k_0 = 2\pi/L_{\max}$ and $k_m = 2\pi/L_{\min}$, $L = L_{\max} - L_{\min}$ being the size of the small chosen section of the flow in the radial direction, chosen to be 2 throughout for these calculations. Similarly, $C_\zeta(\tau)$ and $C_{\mathrm{d}u}(\tau)$ can be easily obtained from equation (7). Note that the choice of constant D_1 and D_2 is due to our primary consideration of the linear perturbation of the flow variables in the presence of an additive noise. However, D_1 and D_2 do not need to always be constant (see [19]). Later, we will discuss the cases with $D \sim k^{-d}$, which effectively does not alter our results.

3.1.1. Asymptotic scaling laws. At large R_e ($\to \infty$) C_u reduces to

$$C_u(\tau)_{R_e\to\infty} \to \frac{8\sqrt{2}\pi^2 q\sqrt{3}}{\sqrt{2-q}}\int_{k_0}^{k_m}\sinh\left(\frac{\sqrt{2(2-q)}}{q\sqrt{3}}\tau\right)\frac{\mathrm{d}k}{k^2} \tag{12a}$$

$$\sim \tau, \quad \text{when } q \to 2 \text{ or } \tau \to 0, \tag{12b}$$

$$\text{but} \quad \sim \exp\left(\frac{\sqrt{2(2-q)}}{q\sqrt{3}}\tau\right) \quad \text{for large } \tau. \tag{12c}$$

Hence, the correlation effectively appears to be independent of q at small and large τ, at large R_e in particular. However, at intermediate τ, correlation diverges at $q \to 2$—when the background specific angular momentum is conserved. Then with the decrease of q, due to the appearance of a fluctuation due to rotational/Coriolis effects with a nonzero epicyclic frequency (see [4, 5] for a detailed discussion), the correlation decreases (see figure 1 also). However, the correlation is effectively controlled by the dynamics of the flow, independent of the viscosity.

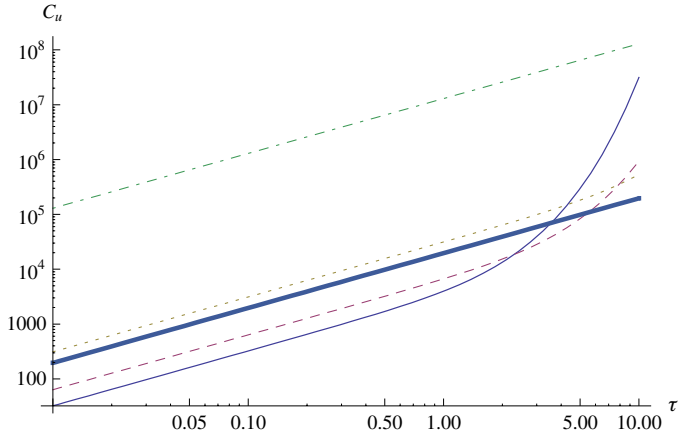

Figure 1. Temporal correlation as a function of time for $R_e = 10\,000$, when $q = 1$ (solid line), 1.5 (dashed line), 1.9 (dotted line), 1.9999 (dot-dashed line) and where the flow is non-rotating (thick line).

For completeness we also calculate the correlation for nonrotating flows, given by

$$C_u(\tau)_{\text{nonrot}} = 8\sqrt{2}\pi^2 R_e \int_{k_0}^{k_m} \frac{\sinh\left(\frac{k^2\tau}{R_e}\right)}{k^4}\,\mathrm{d}k \tag{13a}$$

$$\sim \tau \qquad \text{when } \frac{\tau}{R_e} \ll 1 \tag{13b}$$

$$\sim R_e \qquad \text{when } R_e, \tau \to \infty \tag{13c}$$

$$\sim \frac{\tau^{3/2}}{R_e^{1/2}}\,\text{erfi}\left(k\sqrt{\frac{\tau}{R_e}}\right)\Big|_{k_0}^{k_m} \qquad \text{when } \tau \to \infty \text{ or } \frac{\tau}{R_e} \gg 1. \tag{13d}$$

Hence, unless τ is very small at finite R_e, the correlation depends on R_e—quite an opposite trend to the rotating cases. Interestingly, in the absence of pressure, $C_u(\tau)_{\text{nonrot}} \sim \tau^3$ as $\tau \to \infty$. Therefore, the rotation and pressure both create a significant impact on the behavior in the flow, such that the scaling behavior changes.

Once u_{rms}, $\frac{\partial u_{\text{rms}}}{\partial \vec{x}}$ and ζ_{rms} (when ${A_{\text{rms}}}^2 = |\langle[A(\vec{x}, t+\tau) - A(\vec{x}, t)]^2\rangle| \sim |\langle A(\vec{x}, t)\, A(\vec{x}, t+\tau)\rangle|$, where $A \equiv u$, $\frac{\partial u}{\partial \vec{x}}$, ζ) are known, the evolution of the perturbation energy growth $\mathcal{E} = \frac{1}{8}\left[{u_{\text{rms}}}^2 + \frac{1}{k^2}\left(\frac{\partial u_{\text{rms}}}{\partial \vec{x}}\right)^2 + {\zeta_{\text{rms}}}^2\right]$ can be computed. However, by a simple calculation of the scaling law, it can be shown that each of the terms in $\mathcal{E}$ scales with τ identically and hence the scaling behavior of $\mathcal{E}$ is the same as that of $C_u(\tau)$, apart from a constant factor.

3.1.2. Numerical solutions. Figure 1 shows that with the decrease of q, the temporal correlation of the velocity perturbation decreases as the fluctuation due to the presence of the Coriolis force increases. At small values of q (e.g. for 1, 1.5), however, the Coriolis fluctuation interacting with noise appears to be dominating in a way that the correlation reveals an oscillatory amplitude (this is more clear from figure 2). Hence in a few rotations time the correlation exceeds that of large q, when it increases steadily in the absence of a dominant Coriolis effect at large q. However, in either of the regimes, the temporal correlation of the

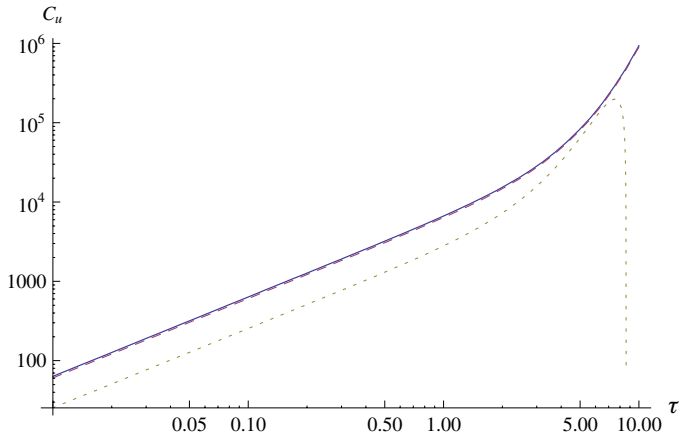

Figure 2. Temporal correlation as a function of time for $q = 1.5$, when $R_e = 10\,000$ (solid line), 1000 (dashed line) and 100 (dotted line).

perturbation appears large enough in a few rotations time, which reveals the nonlinearity in the system, presumably leading to an instability. The correlation appears to be increasing steadily for the nonrotating case, in the absence of Coriolis fluctuation, similar to that for $q \to 2$. Thus the interesting outcome here is the following. The Coriolis fluctuations, along with a steady effect of the noise, lead to a larger $C_u(\tau)$ for a smaller q than that of a larger q in a few rotations time, as is also indicated by equation (12). Note that an important physical quantity in this context is the rotation time of the flow. In a few rotations time, the noise and the Coriolis fluctuation together bring in a large $C_u(\tau)$ and hence a perturbation energy (prone to a smaller q, such as 1.5), which presumably could lead to a transition to turbulence. Therefore, the presence of noise makes the Coriolis effect active to generate instability, which were otherwise acting as an agent hindering the perturbation effects (see, e.g., [4, 5]), leading to a faster rate of perturbation energy growth in the system.

Figure 2 shows that for $q < 2$, the correlation tends to become independent of R_e. This is because with decreasing q, the epicyclic frequency ($\kappa = \Omega\sqrt{2(2-q)}$) becomes larger, bringing a lot of fluctuations in the flow, which makes the flow limited by the dynamics but not by the viscosity. In the absence of noise, the perturbation energy growth (and hence $C_u(\tau)$) is very small, as shown previously [4], for $q < 2$, particularly in three dimensions. Note, however, that at a small/moderate R_e, epicyclic fluctuations work with noise in such a way that $C_u(\tau)$ at small τ appears smaller than that of larger R_e (see $R_e = 100$ case in figure 2) due to the harmonic nature of fluctuations. This effectively argues that the correlation saturates only with the increase of R_e for $q < 2$.

Figure 3 shows that $C_u(\tau)$ for a nonrotating flow at $R_e = 100$ appears larger at large τ compared to that at larger values of R_e. This is due to the effect of noise, which would have been suppressed at larger R_e. This is also clearly understood from the analytical scaling laws given by equation (13). Note that a very large R_e, along with a large τ, diminishes fluctuations in the flow leading to linear perturbation growth with R_e, as shown in equation (13*c*).

Comparing rotating and non-rotating cases, it can be further inferred that the noise suppresses the viscous effects in the rotating flow making it independent of R_e in the regime of smaller τ, as is also shown by equation (12*b*). However, the optimum perturbation of a flow might reveal the correlation varying with R_e, and the above inferences are valid for a fixed perturbation, considered for all the present cases.

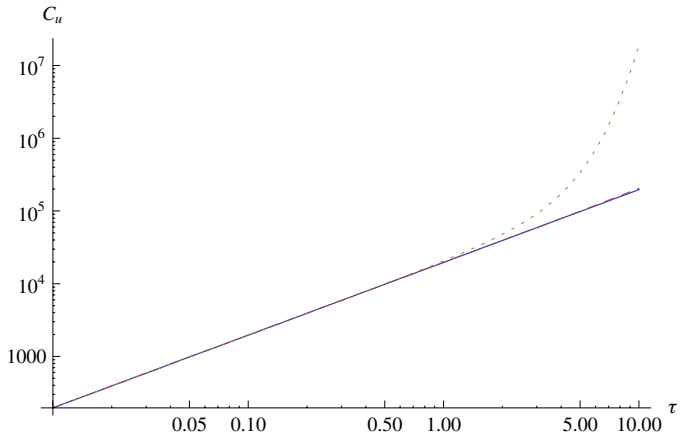

Figure 3. Same as in figure 2, except for a non-rotating flow.

Note that in the absence of noise, perturbation energy growth (and hence $C_u(\tau)$) in all the above rotating cases, essentially for $q < 2$, is very small, as shown previously [4], particularly in three dimensions. However, the effects of noise bring steady growth in the perturbation top of the Coriolis fluctuations. A remarkable feature in the scaling nature of all these correlations, at least for asymptotic τ (see, e.g., equations (12*b*) and (12*c*)), is their independence of q (background angular velocity profile)—a trait identified in statistical physics literature as *universality*. All these flows, with identical overall perturbation energy growth exponents [27] in asymptotic limits of τ (and also R_e), but generally with varying energy dissipation amplitudes, indicate a specific universality class for them.

3.2. Spatial correlation

Here we also assume $\langle \tilde{\eta}_{1\vec{k},\omega}\, \tilde{\eta}_{2\vec{k},\omega} \rangle = 0$ like temporal correlation and obtain spatial correlations of the velocity, vorticity and gradient of the velocity, given below as

$$\begin{aligned}
\langle u(\vec{x},t)\, u(\vec{x}+\vec{r},t)\rangle &= S_u(r) = \int \mathrm{d}^3k\, \mathrm{d}\omega\, \mathrm{e}^{\mathrm{i}\vec{k}.\vec{r}} \langle \tilde{u}_{\vec{k},\omega}\, \tilde{u}_{-\vec{k},-\omega}\rangle,\\
\langle \zeta(\vec{x},t)\, \zeta(\vec{x}+\vec{r},t)\rangle &= S_\zeta(r) = \int \mathrm{d}^3k\, \mathrm{d}\omega\, \mathrm{e}^{\mathrm{i}\vec{k}.\vec{r}} \langle \tilde{\zeta}_{\vec{k},\omega}\, \tilde{\zeta}_{-\vec{k},-\omega}\rangle,\\
\left\langle \frac{\partial u(\vec{x},t)}{\partial x}\, \frac{\partial u(\vec{x}+\vec{r},t)}{\partial x} \right\rangle &= S_{\mathrm{d}u}(r) = \int \mathrm{d}^3k\, \mathrm{d}\omega\, \mathrm{e}^{\mathrm{i}\vec{k}.\vec{r}} k_x^2 \langle \tilde{u}_{\vec{k},\omega}\, \tilde{u}_{-\vec{k},-\omega}\rangle,
\end{aligned} \tag{14}$$

where $\vec{r}$ is the position where the correlations are to be measured.

Now using equations (4), (5), (6) and (14), the velocity correlation perturbation $S_u(r)$ is explicitly given by

$$\begin{aligned}
S_u(r) &= 2\pi \int_{k_0}^{k_m} \mathrm{d}k\, k^2 \int_0^{\pi} d\theta\, \mathrm{e}^{\mathrm{i}kr\cos\theta} \int \mathrm{d}\omega \big[2D_1 q^4 R_e^2 (k^4 + (R_e\omega + LR_e k_y)^2)\\
&\quad + 8D_2 q^2 R_e^4 k_z^2\big] \big/ [4(2-q)^2 R_e^4 k_z^4 + 4R_e^2 q^2 (2-q) k^2 k_z^2 (k^4 - (R_e\omega + LR_e k_y)^2)\\
&\quad + k^4 q^4 (k^4 + (R_e\omega + LR_e k_y)^2)^2]\\
&= 2\pi^2 \int_{k_0}^{k_m} \mathrm{d}k\, k^2 J_0(kr) \int \mathrm{d}\omega \big[2D_1 q^4 R_e^2 (k^4 + (R_e\omega + LR_e k_y)^2)
\end{aligned}$$

$$+ 8D_2q^2R_e^4k_z^2\big]/\big[4(2-q)^2R_e^4k_z^4 + 4R_e^2q^2(2-q)k^2k_z^2(k^4 - (R_e\omega + LR_ek_y)^2)$$
$$+ k^4q^4(k^4 + (R_e\omega + LRk_y)^2)^2\big], \tag{15}$$

where $J_0(kr)$ is the zeroth-order Bessel function. Similarly, one can obtain $S_\zeta(r)$ and $S_{\mathrm{d}u}(r)$ explicitly, when the poles in equation (15) are exactly the same as that given by equation (9). Here we also stick to the simplifying assumption $k_x = k_y = k_z = k/\sqrt{3}$.

Now following the same procedure as was applied for the correlation of the temporal velocity perturbation, we obtain the correlation of the spatial velocity perturbation $S_u(r)$ given by

$$S_u(r) = \int_{k_0}^{k_m} \mathrm{d}k k^2 J_0(kr)\mathrm{RES}_{S_u}(q, R_e, r), \tag{16}$$

where $\mathrm{RES}_{S_u}(q, R_e, r)$ is the magnitude of the part arising from the frequency integration.

3.2.1. Asymptotic scaling laws. At large r and R_e (which is a natural/astrophysical scenario), the flows with all q reveal identical scaling of the correlation with r given by

$$S_{u\,(R_e \text{ and } r\to\infty)} \to \frac{\pi^{3/2}q}{r^{1/2}}\,(2-q)^{-3/2}\int_{k_0}^{k_m}\mathrm{d}k\,\exp(-kr)\,\frac{2\sqrt{3}(k^2-1)+q\sqrt{3}}{k^{5/2}} \tag{17}$$

which is independent of R_e. Note that at finite r, $\exp(-kr)/\sqrt{r} \to J_0(kr)$. Hence, the flow is limited by the dynamics. This reveals identical roughness exponents [27] for all flows, indicating a single universality class, as was already predicted from the temporal correlations. Equation (17) also reveals a steadily damped instability. It further recovers the fact that the flow exhibits an unbounded correlation as $q \to 2$, and hence unbounded growth of the perturbation. At small r

$$S_{u\,(R_e\to\infty,\ r\to 0)} \to -q\,(2-q)^{-3/2}\int_{k_0}^{k_m}\mathrm{d}k\,\frac{(2-q-2k^2)\log\left(\frac{kr}{2}\right)}{k^2}, \tag{18}$$

which is again determined by the rotational parameter q only, when $\log(kr/2)$ becomes negative at small r. Hence, except when $q = 2$ (or when q is very very close to 2) and/or when $r = 0$ (or when r is very very close to 0), the correlation is finite.

For completeness, we also describe the scaling laws for nonrotating flows. At large r and R_e

$$S^{\text{nonrot}}_{u\,(R_e \text{ and } r\to\infty)} \to \frac{R_e\,\pi^{3/2}\sqrt{2}}{r^{1/2}}\int_{k_0}^{k_m}\mathrm{d}k\,\frac{\exp(-kr)}{k^{9/2}}, \tag{19}$$

which scales with R_e, unlike the rotating flows. Hence the flow is not limited by the dynamics at any r. However, at $r \to 0$ the scaling behavior changes and is given by

$$S^{\text{nonrot}}_{u\,(R_e\to\infty,\ r\to 0)} \to -2R_e\pi\int_{k_m}^{k_0}\mathrm{d}k\,\frac{\log\left(\frac{kr}{2}\right)}{k^4}, \tag{20}$$

which still scales linearly with R_e.

3.2.2. Numerical solutions. Figures 4 and 5 show that the spatial correlations of the perturbation decrease with the decrease of q from 2, when the epicyclic fluctuations arise in the flow. Moreover, the correlations for all R_e tend to merge at large r, at a given q particularly, becoming independent of R_e, as is also shown by the asymptotic result given by equation (17). However, at small r and finite R_e, they depend on the viscosity. This is due to the effect of the noise, as is the case for temporal correlations.

On the other hand, for non-rotating flows, the correlations are not limited by the dynamics of the flow, as shown by figure 6, rather they are controlled by the viscosity. This is also

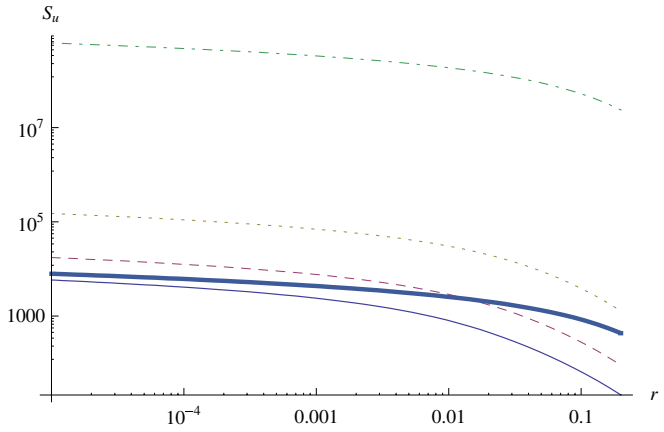

Figure 4. Spatial correlation as a function of radial coordinate for $R_e = 10\,000$, when $q = 1$ (solid line), 1.5 (dashed line), 1.9 (dotted line), 1.9999 (dot-dashed line) and the flow is non-rotating (thick line).

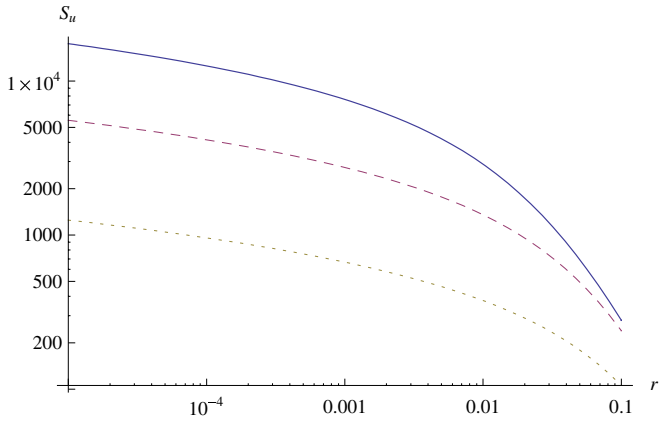

Figure 5. Spatial correlation as a function of radial coordinate for $q = 1.5$, when $R_e = 10\,000$ (solid line), 1000 (dashed line) and 100 (dotted line).

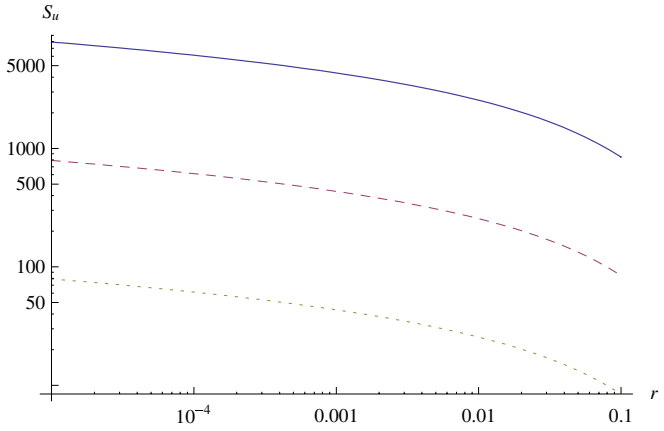

Figure 6. Same as in figure 5, except for non-rotating flow.

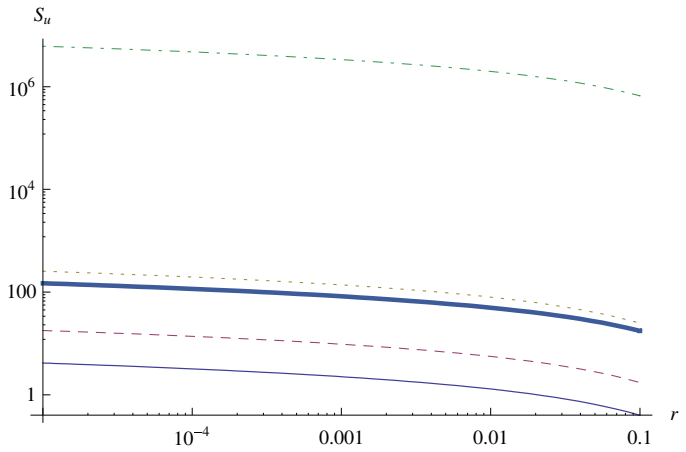

Figure 7. Same as in figure 4, except for $D_1 = D_2 \sim 1/k^3$.

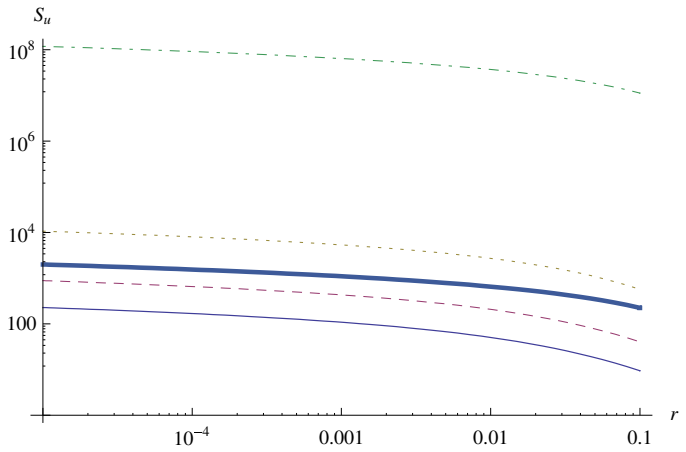

Figure 8. Same as in figure 4, except for $D_1 = D_2 \sim 1/k$.

understood from equations (19) and (20). Hence, the rotational effects constrain the correlation noticeably.

It is generally seen that the correlations decrease with increasing r and decreasing q. Note their exponential decaying nature in equations (17) and (19) compared to the logarithmic variance in equations (18) and (20). However, their values appear significant enough to reveal a steadily damped instability in the flow. The possibilities of steadily damped oscillatory instabilities in constrained Orr–Sommerfeld flows were already predicted in two dimensions [39] as well as in the recirculating cavities between the jets produced behind a high solidity grid consisting of a perforated plate [40].

All the above correlations are computed for white noise. Figures 7 and 8 show the variations of the spatial correlations of the velocity perturbation for color noise respectively without and with vertex corrections in $D_i(k)$. Interestingly, while the magnitude of correlations decreases with respect to that for white noise (particularly for $D_1 = D_2 \sim 1/k^3$), with the increase of q they appear large enough to govern instability. As an example, for noise with

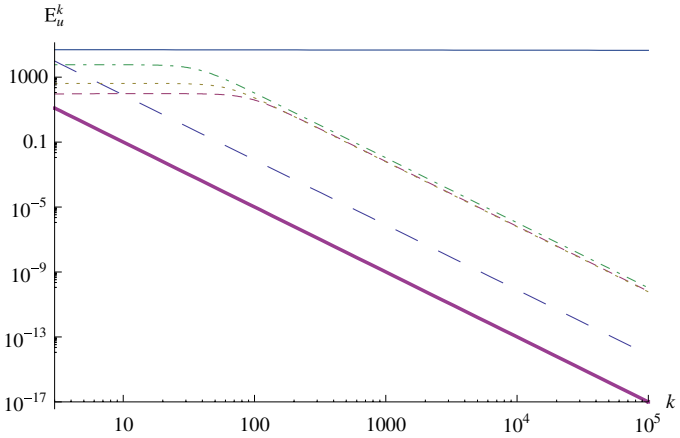

Figure 9. Energy spectra for the velocity perturbation, when $q = 1$ (dashed line), 1.5 (dotted line) and 1.9 (dot-dashed line) and the flow is nonrotating (longdashed). The solid and thick-solid lines respectively indicate the nature of the slope of the curves at small and large k for rotating flows. $D_1 = D_2 = 1$, $R_e = 10\,000$.

vertex correction, the Keplerian flow still reveals a large enough correlation even at small radial coordinates.

All the above large values of the perturbation energy growth are indicative of pure hydrodynamic instability and plausible turbulent transport, which is one of the outcomes from this theory.

3.3. Spectrum

In order to compute the spectrum of the flow, let us first integrate the ω-part of equation (15) and obtain

$$\int E_u(k)\mathrm{d}k = \int \mathrm{d}^3k\,\mathrm{RES}_{S_u}(q, R_e, k, D_1, D_2). \tag{21}$$

Similarly, one can obtain $\int E_\zeta(k)\,\mathrm{d}k$ and $\int E_{\mathrm{d}u}(k)\,\mathrm{d}k$ from S_ζ and $S_{\mathrm{d}u}$ respectively. They would scale in the same way as of $\int E_u(k)\mathrm{d}k$. Hence, the energy spectrum can generally be given by

$$E_u(k) = Ck^2\,\mathrm{RES}_{S_u}(q, R_e, k, D_1, D_2), \tag{22}$$

when C is a constant. Figures 9 and 10 show that the energy spectra for all the rotating flows with $q < 2$ have the same spectral indices at large and small k. Moreover, the energy appears identical for all q at large k, which is due to the fact that a small length scale appears identical for all rotational profiles. On the large scale, the spectral index is the same as that of the noise correlation, which implies that the flow is controlled by the noise in that regime. However, interestingly, there is no change of slope in the nonrotating case, and the corresponding power-law index appears the same as that of the large k rotating ones. This may be understood as the Coriolis force in the rotating flows distorting the system, which results in affecting the large scale (and hence small k) behavior of the flow. Hence, the behavior of a non-rotating flow appears the same throughout without being affected by the rotational effects. Note also that the color noise increases the power-law indices throughout compared to that for white noise.

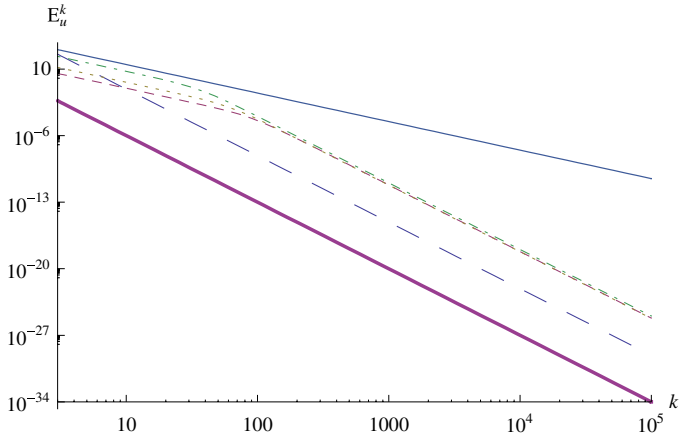

Figure 10. Same as in figure 9, except for $D_1 = D_2 \sim 1/k^3$.

4. Summary and conclusion

We have attempted to address the origin of instability and then turbulence in rotating shear flows (more precisely a small section of one, which is a plane shear flow with the Coriolis force). Our particular emphasis is the flows having angular velocity decreasing but specific angular momentum increasing with the radial coordinate, which are Rayleigh stable. The flows with such kinds of velocity profiles are often seen in astrophysics. As the molecular viscosity in astrophysical accretion discs is negligible, any transport of the matter therein would arise through turbulence. However, the Rayleigh stable flows, particularly in the absence of magnetic coupling, could not reveal any unstable mode which could serve as a seed of turbulence. Therefore, essentially we have addressed the plausible origin of *pure hydrodynamic turbulence* in rotating shear flows of the kind mentioned above. This is particularly meaningful for charged natural flows like accretion discs around quiescent cataclysmic variables, in protoplanetary and star-forming discs, and the outer region of discs in active galactic nuclei etc, where flows are cold and of low ionization and are effectively neutral in charge. Note that whether a flow is magnetically arrested or not, the magnetic instability is there or not, hydrodynamic effects always exist. Hence, the relative strengths of hydrodynamics and hydromagnetics in the time scale of interest determine the actual source of the instability.

We have shown, based on the theory of statistical physics, that stochastically forced linearized rotating shear flows in a narrow gap limit reveal a large correlation energy growth of the perturbation in the presence of noise. While the correlations are directly proportional to the Reynolds number for nonrotating flows, they are independent of or weakly dependent on the Reynolds number for rotating flows. Hence the later flows are mostly controlled by the dynamics and the noise. While correlations of the perturbation decrease as the flow deviates from the type of constant specific angular momentum, to the Keplerian and then to constant circular velocity, still they appear large enough to trigger nonlinear effects and instability.

While earlier the origin of hydrodynamic instability in rotating shear flows of this kind was addressed based on the 'bypass method' in two dimensions [4, 5], it was shown that [15] extra physics, e.g. elliptical vortex effects, have to be invoked for such instabilities to occur in three dimensions. However, later theories showing instabilities are effectively based on nonlinear theory. Therefore, this work addresses the *large three-dimensional hydrodynamic energy growth of linear perturbation* for the first time, in such rotating flows, to the best of

our knowledge, which presumably leads to the instability and subsequent turbulence in such flows. The only requirement here is to have the presence of stochastic noise in the system, which is quite obvious in natural flows like astrophysical accretion discs. Indeed, to the best of our knowledge, no one so far has addressed the effects of stochastic noise in such rotating flows.

Interestingly, the flows with the velocity profile $\Omega \sim r^{-q}$, with $q < 2$, exhibiting identical overall growth exponents (but maybe not identical energy dissipation amplitudes), indicate a specific universality class. At large r, they also reveal identical roughness exponents. Thus the properties of temporal and spatial correlations together indicate the Rayleigh stable rotating shear flows follow a single universality class.

Let us end by clarifying the suitability of an astrophysical application of our results, which is based on an incompressible assumption. If the wavelength of the velocity perturbations is much shorter than the sound horizon for the time of interest (e.g. infall time of matter), then the density perturbations (i.e. the sound waves) reach equilibrium early on, exhibiting effectively a uniform density during the timescale of interest. For a geometrically thin astrophysical accretion disc around a gravitating mass, the vertical half-thickness of the disc (h) is comparable to the sound horizon corresponding to one disc rotation time [41] such that $h \sim c_s/\Omega$. Therefore, as described in previous work [1, 3, 5, 16, 42, 43], for processes taking longer than one rotation time, wavelengths shorter than the disc thickness can be approximately treated as incompressible. A detailed astrophysical application of this work has been reported elsewhere [44].

Acknowledgments

The authors would like to thank Rahul Pandit for discussion. Thanks are also due to the referees for carefully reading through the paper and the various suggestions which have helped to improve the presentation of the work. This work is partly supported by a project, grant no. ISRO/RES/2/367/10-11, funded by ISRO, India.

Appendix. Magnetic version of the set of Orr–Sommerfeld and Squire equations

Let us now establish the linearized Navier–Stokes equation in the presence of background plane shear $(0, -x, 0)$ without neglecting magnetic coupling with a background magnetic field $(0, B_1, 1)$, when B_1 is a constant, in the presence of angular velocity $\Omega \sim r^{-q}$ in a small section of the incompressible flow. Hence, the underlying equations are nothing but the linearized set of hydromagnetic equations including the equations of induction in the local Cartesian coordinates (see, e.g., [4, 10] for a detailed description of the choice of coordinate in a small section) given by

$$\left(\frac{\partial}{\partial t} - x\frac{\partial}{\partial y}\right)u - \frac{2v}{q} + \frac{\partial p_{\rm tot}}{\partial x} - \frac{1}{4\pi}\left(B_1\frac{\partial B_x}{\partial y} + \frac{\partial B_x}{\partial z}\right) = \frac{1}{R_e}\nabla^2 u, \tag{A.1}$$

$$\left(\frac{\partial}{\partial t} - x\frac{\partial}{\partial y}\right)v + \left(\frac{2}{q} - 1\right)u + \frac{\partial p_{\rm tot}}{\partial y} - \frac{1}{4\pi}\left(B_1\frac{\partial B_y}{\partial y} + \frac{\partial B_y}{\partial z}\right) = \frac{1}{R_e}\nabla^2 v, \tag{A.2}$$

$$\left(\frac{\partial}{\partial t} - x\frac{\partial}{\partial y}\right)w + \frac{\partial p_{\rm tot}}{\partial z} - \frac{1}{4\pi}\left(B_1\frac{\partial B_z}{\partial y} + \frac{\partial B_z}{\partial z}\right) = \frac{1}{R_e}\nabla^2 w, \tag{A.3}$$

$$\frac{\partial B_x}{\partial t} = \frac{\partial u}{\partial z} + B_1\frac{\partial u}{\partial y} + x\frac{\partial B_x}{\partial y} + \frac{1}{R_m}\nabla^2 B_x, \tag{A.4}$$

$$\frac{\partial B_y}{\partial t} = \frac{\partial v}{\partial z} + B_1 \frac{\partial v}{\partial y} - x\frac{\partial B_x}{\partial x} - x\frac{\partial B_z}{\partial z} - B_x + \frac{1}{R_m}\nabla^2 B_y, \tag{A.5}$$

$$\frac{\partial B_z}{\partial t} = \frac{\partial w}{\partial z} + B_1 \frac{\partial w}{\partial y} + x\frac{\partial B_z}{\partial y} + \frac{1}{R_m}\nabla^2 B_z, \tag{A.6}$$

when the vectors for the velocity and magnetic field perturbations are (u, v, w) and (B_x, B_y, B_z) respectively, R_e and R_m are the hydrodynamic and magnetic Reynolds numbers respectively and $p_{\rm tot}$ is the total pressure perturbation (including that due to the magnetic field). The above equations are supplemented by the conditions for incompressibility and no magnetic charge, given by

$$\frac{\partial u}{\partial x} + \frac{\partial v}{\partial y} + \frac{\partial w}{\partial z} = 0, \tag{A.7}$$

$$\frac{\partial B_x}{\partial x} + \frac{\partial B_y}{\partial y} + \frac{\partial B_z}{\partial z} = 0. \tag{A.8}$$

Now by taking partial derivatives with respect to x, y, z respectively on both sides of equations (A.1), (A.2), (A.3) and adding them up we obtain

$$\nabla^2 p_{\rm tot} = \frac{2}{q}\left(\frac{\partial v}{\partial x} - \frac{\partial u}{\partial y}\right) + 2\frac{\partial u}{\partial y}. \tag{A.9}$$

Now taking ∇^2 to equation (A.1), using equation (A.9) and defining the x-component of vorticity $\zeta = \partial w/\partial y - \partial v/\partial z$, we obtain

$$\left(\frac{\partial}{\partial t} - x\frac{\partial}{\partial y}\right)\nabla^2 u + \frac{2}{q}\frac{\partial \zeta}{\partial z} - \frac{1}{4\pi}\left(B_1\frac{\partial}{\partial y} + \frac{\partial}{\partial z}\right)\nabla^2 B_x = \frac{1}{R_e}\nabla^4 u. \tag{A.10}$$

Also by taking partial derivatives with respect to x and y respectively on both sides of equations (A.2) and (A.1) respectively, subtracting one from the other and defining $\zeta_B = \partial B_z/\partial y - \partial B_y/\partial z$, we obtain

$$\left(\frac{\partial}{\partial t} - x\frac{\partial}{\partial y}\right)\zeta + \left(1 - \frac{2}{q}\right)\frac{\partial u}{\partial z} - \frac{1}{4\pi}\left(B_1\frac{\partial}{\partial y} + \frac{\partial}{\partial z}\right)\zeta_B = \frac{1}{R_e}\nabla^2\zeta. \tag{A.11}$$

Furthermore, by taking partial derivatives with respect to y and z respectively on both sides of equations (A.6) and (A.5) and subtracting one from the other, we obtain

$$\left(\frac{\partial}{\partial t} - x\frac{\partial}{\partial y}\right)\zeta_B = \frac{\partial \zeta}{\partial z} + B_1\frac{\partial \zeta}{\partial y} + \frac{\partial B_x}{\partial z} + \frac{1}{R_m}\nabla^2\zeta_B. \tag{A.12}$$

The equations (A.10), (A.11), (A.4) and (A.12) describe the magnetized version of the set of the Orr–Sommerfeld and Squire equations in the presence of the Coriolis force, for the background magnetic field described above and linear shear. To the best of our knowledge, this set of equations has not been reported in the existing literature so far.

References

[1] Chagelishvili G D, Zahn J P, Tevzadze A G and Lominadze J G 2003 *Astron. Astrophys.* **402** 401
[2] Tevzadze A G, Chagelishvili G D, Zahn J P, Chanishvili R G and Lominadze J G 2003 *Astron. Astrophys.* **407** 779
[3] Yecko P A 2004 *Astron. Astrophys.* **425** 385
[4] Mukhopadhyay B, Afshordi N and Narayan R 2005 *Astrophys. J.* **629** 383
[5] Afshordi N, Mukhopadhyay B and Narayan R 2005 *Astrophys. J.* **629** 373
[6] Butler K M and Farrell B F 1992 *Phys. Fluids* **4** 1637
[7] Reddy S C and Henningson D S 1993 *J. Fluid Mech.* **252** 209

[8] Trefethen L N, Trefethen A E, Reddy S C and Driscoll T A 1993 *Science* **261** 578
[9] Farrell B F 1988 *Phys. Fluids* **31** 2093
[10] Mukhopadhyay B, Mathew R and Raha S 2011 *New J. Phys.* **13** 023029
[11] Ji H, Burin M, Schartman E and Goodman J 2006 *Nature* **444** 343
[12] Paoletti M S and Lathrop D P 2011 *Phys. Rev. Lett.* **106** 024501
[13] Avila M 2012 *Phys. Rev. Lett.* **108** 124501
[14] Mukhopadhyay B and Saha K 2011 *Res. Astron. Astrophys.* **11** 163
[15] Mukhopadhyay B 2006 *Astrophys. J.* **653** 503
[16] Rajesh S R 2011 *Mon. Not. R. Astron. Soc.* **414** 691
[17] Chandrasekhar S 1961 *Hydrodynamics and Hydromagnetic Stability* (Oxford: Oxford University Press)
[18] Batchelor G K 2000 *An Introduction to Fluid Mechanics* (Cambridge: Cambridge University Press)
[19] Forster D, Nelson D R and Stephen M J 1977 *Phys. Rev.* A **16** 732
[20] De Dominicis C and Martin P C 1979 *Phys. Rev.* A **19** 419
[21] Kolmogorov A N 1941 *Dokl. Akad. Nauk SSSR* **30** 301
[22] Kolmogorov A N 1962 *J. Fluid Mech.* **13** 82
[23] Bhattacharjee J K 1996 *Phys. Rev. Lett.* **77** 1524
[24] Kardar M, Parisi G and Zhang Y-C 1986 *Phys. Rev. Lett.* **56** 889
[25] Chekhlov A and Yakhot V 1995 *Phys. Rev.* E **51** 2739
[26] Chattopadhyay A K and Bhattacharjee J K 1998 *Europhys. Lett.* **42** 119
[27] Barabási A-L and Stanley H E 1995 *Fractal Concepts in Surface Growth* (Cambridge: Cambridge University Press)
[28] Medina E, Hwa T, Kardar M and Zhang Y-C 1989 *Phys. Rev.* A **39** 3053
[29] Chattopadhyay A K and Bhattacharjee J K 2001 *Phys. Rev.* E **63** 016306
[30] Landau L D and Lifshitz E M 1987 *Fluid Mechanics* (*Course of Theoretical Physics* vol 6) (Portsmouth, NH: Butterworth-Heinemann)
[31] Jacobi I and Mckeon B J 2011 *J. Fluid Mech.* **677** 179
[32] Meneveau C and Katz J 2000 *Ann. Rev. Fluid Mech.* **32** 1
[33] Mukhopadhyay B 2009 *Astrophys. J.* **694** 387
[34] Misra R, Harikrishnan K P, Mukhopadhyay B, Ambika G and Kembhavi A K 2004 *Astrophys. J.* **609** 313
[35] Karak B B, Dutta J and Mukhopadhyay B 2010 *Astrophys. J.* **715** 697
[36] Rajesh S R and Mukhopadhyay B 2010 *Mon. Not. R. Astron. Soc.* **402** 961
[37] Mukhopadhyay B and Ghosh S 2003 *Mon. Not. R. Astron. Soc.* **342** 274
[38] Balbus S A and Hawley J F 1991 *Astrophys. J.* **376** 214
[39] Akhavan R, Kamm R D and Shapiro A H 1991 *J. Fluid Mech.* **225** 423
[40] Villermaux E, Gagne Y, Hopfinger E J and Sommeria J 1991 *Eur. J. Mech.* B **10** 427
[41] Pringle J E 1981 *Annu. Rev. Astron. Astrophys.* **19** 137
[42] Johnson B M and Gammie C F 2005 *Astrophys. J.* **635** 149
[43] Umurhan O M, Menou K and Regev O 2007 *Phys. Rev. Lett.* **98** 034501
[44] Mukhopadhyay B and Chattopadhyay A K 2012 *Proc. Int. Conf. on Astrophysics and Cosmology (Tribhuvan University, Kirtipur, Nepal, 19–21 March)*